Article Identifier
DOI: 10.22032/dbt.58889
URN: urn:nbn:de:gbv:ilm1-2023isc-042:2

60th ILMENAU SCIENTIFIC COLLOQUIUM
Technische Universität Ilmenau, 4 – 8 September 2023
URN: urn:nbn:de:gbv:ilm1-2023isc:1

DESIGN OF THE COMPOUND COMPLIANT SCOTT-RUSSEL MECHANISM WITH NON-CONVENTIONAL OPTIMIZATION OF FLEXURE HINGES

Dušan Stojiljković, Nenad T. Pavlović

Faculty of Mechanical Engineering, University of Niš, A. Medvedeva 14, 18000 Niš, Serbia

ABSTRACT

Compliant mechanisms gain some or all their mobility from the relative flexibility of their joints rather than from rigid-body joints only. Compliant mechanisms can provide many benefits in the solution of design problems: they have less wear, weight, noise, and backlash than their rigid-body counterparts. They can be manufactured from one piece of material, and therefore they are suitable to be applied in micromechanics. However, nonlinearities introduced by the large deflection of elastic segments further complicate the analysis of compliant mechanisms. This paper considers the isosceles slider–crank mechanism and its compliant counterpart mechanism, being developed based on the rigid–body mechanism. The design of the compound compliant slider-crank mechanism with circular flexure hinges notch, consisting of two single compliant slider-crank mechanisms has been shown in this paper. The guiding accuracy and mobility of the newly designed compliant mechanism have been analyzed. Additionally, by using undercut notch flexure hinges, a new analysis is given, which aims to show another factor that has an impact on the operation of compliant mechanisms. This factor is represented by the position of joints and its influence is shown through improving the accuracy of the coupler point rectilinear path of the Scott-Russel mechanism. Hence, it will be described that the position of these flexure hinges and their geometry is a vital issue for performing an approximately rectilinear path. Therefore, several designs are investigated through the finite elements method (FEM) simulation.

Index Terms - Compliant mechanisms, Flexure hinges, Scott-Russel mechanism, Coupler point guiding, FEA optimization

1. INTRODUCTION

While the most basic requirement for every engineering solution is functionality, another requirement that has greatly increased in relevance over the past few decades is the optimality of the solution. Such a proposal is in line with the general need for resource and energy sustainability. The optimality criteria of an engineering solution depend on a wide range of factors, including the application domain, required service life, available time, development tools, etc. As a result, engineers work hard to come up with creative approaches to make their solutions better in terms of many parameters. Numerous advancements, many of which center on mechanisms, are targeted toward achieving this goal. These include mechanisms' working space analysis and optimization [1-3], the design and topology optimization of mechanisms in relation to the used production procedures [4-6], and the use of novel, lightweight materials [7-9].

The relative flexibility of the joints of compliant mechanisms contributes to some of their mobility rather than relying only on rigid-body joints. Flexure hinges provide many advantages when used in mechanism construction, including the ability to build a mechanism as a single piece, reduced weight the absence of lubrication requirements, and the elimination of wear, clearance, friction, and noise. They can consequently be used for micromachining. Compliant mechanisms and actuators are becoming more and more crucial due to their benefits in robotics, medical technology, sensor application, and managing compressible objects [10]. On the other hand, the flexure hinged mechanisms have limited mobility, or the capacity to realize small displacements.

The design and function of flexure hinge and mechanisms have been extensively studied. The basic language and classification for the parts of compliant mechanisms have been defined by several authors [1–13]. A comparison of the designing process for a class of compliant mechanisms with a relatively small flexible part and relatively rigid sections of the mechanism has also been suggested [12, 14]. The homogenization method has been introduced by Ananthasuresh and Kota [15] as a formal structural optimization tool for developing flexible structures. Böttcher et al. [16] developed motion task elastically movable structures for positioning and manipulation in engineering based on the innovative ideas of technically possible joints from nature.

Pavlović et al. [17–20] have looked at how the geometry and material of the flexure hinges affect the precision of some of their guiding points.

Pavlović and Pavlović [21] introduced the basic compliant mechanism concept for axial link translation.

Pavlović and Stojiljković [22] have looked at the accuracy with which compliant cognate mechanisms are based on Watt's linkage guide behavior.

To enhance the dynamic performance of the intelligent excavation process, Yuan et al. [23] created the rigid-flexible coupling virtual prototyping model of the excavator attachment.

Stojiljković et al. [24] explore influence of the undercut flexure hinge position through improving the accuracy of the coupler point rectilinear path of the Roberts-Chebyshev cognate compliant mechanism.

The kinematics approach and the structural optimization approach are typically used to build compliant machines. In this research, the kinematics approach—a compliant mechanism created as the rigid-body linkage's counterpart, capable of performing the desired function—has been applied.

The Scott-Russel mechanism, an isosceles slider-crank mechanism created based on the rigid-body mechanism, is discussed in this study along with its compliant counterpart mechanism. The paper aims to present the results of structural analysis and position optimization as a tool for obtaining the best results of the initially designed compliant Scott-Russel mechanism regarding guiding accuracy (minimal difference between the realized path of the "coupler" point and the exact straight line). The guiding accuracy and mobility of the newly designed compliant mechanism have been analyzed. For this analysis two types of compliant joints were used: circular notch flexure hinges as well as undercut flexure hinges. The analysis of joints usually points to the use of different dimensions, materials, and shapes of flexure hinges to obtain the best output parameters of the compliant mechanism that is designed and modeled. By using undercut notch flexure hinges, a new analysis is given, which aims to show another factor that has an impact on the operation of compliant mechanisms. This factor is represented by the position of joints and its influence is shown through improving the accuracy of the coupler point rectilinear path of the Scott-Russel mechanism. Hence, it will be described that the position of these flexure hinges and their geometry is a vital issue for performing an approximately rectilinear path. Therefore, several designs are investigated through the finite elements method (FEM) simulation.

2. THE SINGLE COMPLIANT SCOTT-RUSSEL MECHANISM

A rigid-body Scott-Russel mechanism is depicted in Fig. 1 (the isosceles slider-crank mechanism: $a = \overline{A_0A} = \overline{AB} = \overline{AC}$). The coupler point C is directed in a precise vertical rectilinear route.

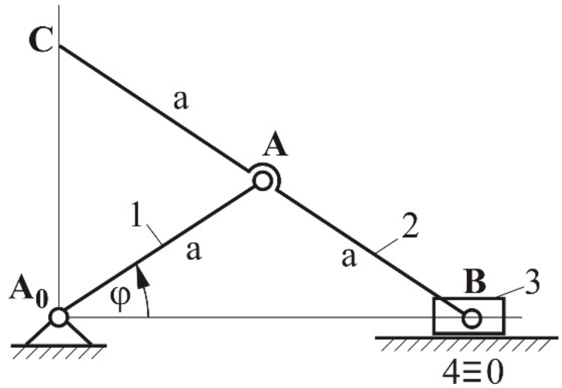

Fig. 1. A rigid-body Scott-Russel mechanism

Based on the rigid-body Scott-Russel mechanism, a compliant Scott-Russel mechanism with flexure hinges designed as circular flexure hinges will be developed.

Fig. 2 shows a circular flexure hinge notch as a characteristic type of the flexure hinge. This flexure hinge is fully determined by two parameters: the width of relatively rigid segments w_R and the width of relatively elastic segments w_E.

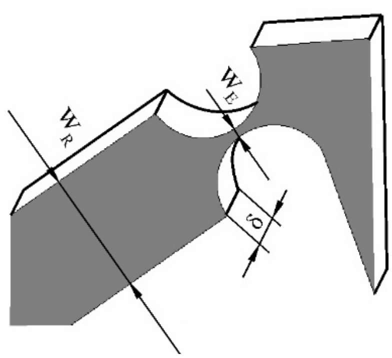

Fig. 2: A flexure hinge with a circular notch

Based on the rigid-body Scott-Russel mechanism, a compliant Scott-Russel mechanism with notch joints was developed (Fig. 3a). The flexure hinges A_0 and A have been oriented in the direction of the rigid-body input crank A_0A, while the flexure hinge B has been oriented in the direction of the rigid-body coupler CAB. Three different variants of the input force have been denoted with F_a, F_b, and F_c. The deformed and undeformed position of the compliant slider-crank mechanism with notch joints is shown in Fig. 3b.

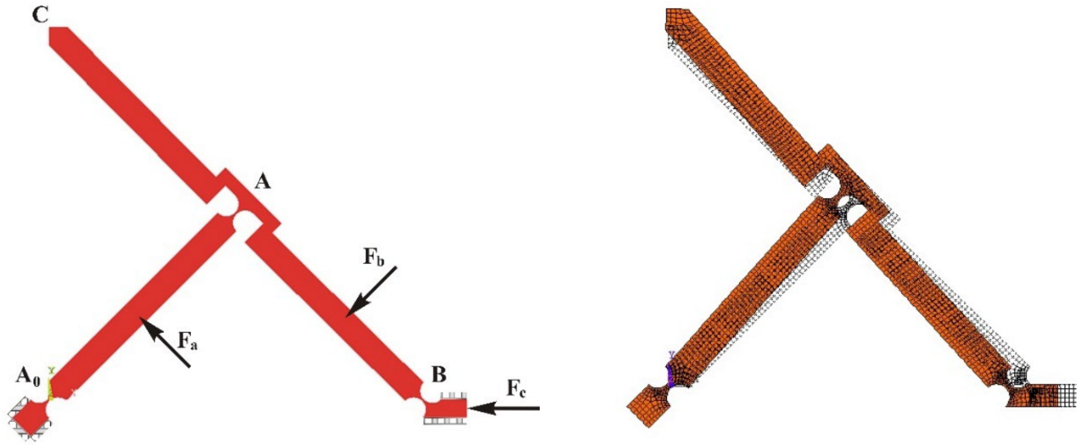

Fig. 3: The compliant Scott-Russel mechanism with notch flexure hinges: (a) Boundary conditions with acting forces, (b) Deformed and undeformed position of compliant mechanism with element mesh

The symmetrical axes of the compliant notch joints cross each other at the point 1 (Fig. 4) corresponding to the revolute joint of the rigid-body counterpart. The other characteristic key points of a compliant notch joint (Fig. 4) can be calculated by using the set of equations:

$$\overrightarrow{r_2} = \overrightarrow{r_1} + \frac{w_R}{2} e^{i\left(\phi - \frac{\pi}{2}\right)} \quad (4a)$$

$$\overrightarrow{r_3} = \overrightarrow{r_2} + \frac{w_R - w_E}{2} e^{i\phi} \quad (4b)$$

$$\overrightarrow{r_4} = \overrightarrow{r_3} + \frac{w_R - w_E}{2} e^{i(\phi - \pi)} \quad (4c)$$

$$\overrightarrow{r_5} = \overrightarrow{r_4} + \frac{w_R - w_E}{2} e^{i\left(\phi + \frac{\pi}{2}\right)} \quad (4d)$$

$$\overrightarrow{r_6} = \overrightarrow{r_1} + \frac{w_R}{2} e^{i\left(\phi + \frac{\pi}{2}\right)} \quad (4e)$$

$$\overrightarrow{r_7} = \overrightarrow{r_6} + \frac{w_R - w_E}{2} e^{i\phi} \quad (4f)$$

$$\overrightarrow{r_8} = \overrightarrow{r_6} + \frac{w_R - w_E}{2} e^{i(\phi - \pi)} \quad (4g)$$

$$\overrightarrow{r_9} = \overrightarrow{r_6} + \frac{w_R - w_E}{2} e^{i\left(\phi - \frac{\pi}{2}\right)} \quad (4h)$$

ϕ

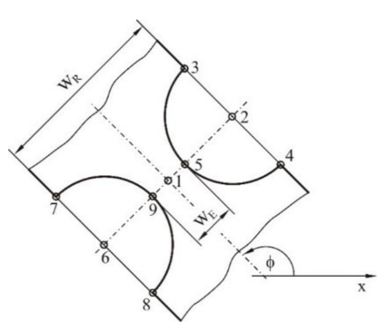

Fig. 4: Characteristic key points of a flexure hinge notch

3. THE GUIDING ACCURACY OF THE SINGLE COMPLIANT SCOTT-RUSSEL MECHANISM

We have analyzed the "coupler" point guiding accuracy (on the rectilinear trace of $\Delta y_C = 5$ mm) of the compliant Scott-Russel mechanism with notch joints. The values of the lengths of the mechanism have been $a = \overline{A_0A} = \overline{AB} = 50\ mm$, the initial position of the "input crank" has been $\varphi = 45^o$, while the following flexure hinge parameters have been assumed: relatively rigid segments width $w_R = 5$ mm and relatively elastic segments width $w_E = 0.5$ mm.

The position analysis of the compliant mechanisms was performed using the ANSYS software. It has been assumed that the compliant mechanisms are made of material piacryl with the properties: Young's modulus E = 3700 N/mm^2, flexural strength $\sigma_{bs} = 90$ N/mm^2, the thickness of material $\delta = 4$ mm. A characteristic ANSYS element type PLANE 183 (2-D 8-Node Structural Solid) has been used to perform the calculation for rectangular cross-sectional area elements.

The guiding accuracies were compared for three different cases of the location of the acting point of input load force: in the middle of the "input crank" - F_a, in the middle of the "coupler" AB - F_b, and the slider - F_c (Fig. 3a). This is because the input load force acting point does not necessarily have to be located on the compliant mechanism's "input crank" only.

The results have been shown in Table 1.

Table 1. Guiding accuracy of the single-compliant Scott-Russel mechanisms

Guiding accuracy Δx_C [µm] on the vertical displacement of Δy_C = 5 mm		
Input force case F_a	Input force case F_b	Input force case F_c
168.6	92.6	204.3

The compliant Scott-Russel mechanism with the acting point of input load force situated in the middle of the "coupler" AB has provided the best-guiding accuracy (minimum variation between absolute rectilinear and realized trace) of the "coupler" point on the rectilinear trace.

4. THE GUIDING ACCURACY OF THE COMPOUND COMPLIANT SCOTT-RUSSEL MECHANISM

The compound structure of the Scott-Russel compliant mechanism was designed to improve guiding accuracy. We have added to the above-mentioned single compliant mechanism another the same compliant mechanism as a mirror image. These single compliant mechanisms have been rigidly connected at the guided coupler point.

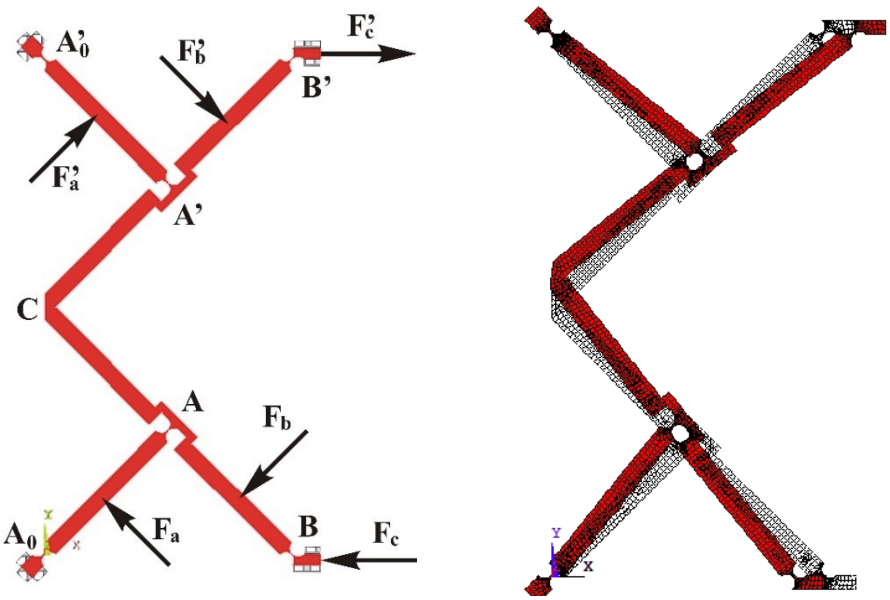

Fig. 5: The compliant compound Scott-Russel mechanism with notch flexure hinges: (a) Boundary conditions with acting forces, (b) Deformed and undeformed position of compliant mechanism with element mesh

The compliant compound mechanism has been actuated by two simultaneous input forces, where each input force act on the single compliant mechanism. The guiding inaccuracies of both single compliant mechanisms compensate each other producing better guiding accuracy of the compound compliant mechanism. In other words, the compliant compound mechanism can provide better guiding accuracy than the respective single compliant mechanism.

The guiding accuracies were compared for three different cases of the location of the acting points of input load forces: in the middle of the "input crank" - F_a and F'_a, in the middle of the "coupler" AB - F_b and F'_b, and in the slider - F_c and F'_c (Fig. 5a).

The results have been shown in Table 2.

Table 2. Guiding accuracy of the Scott-Russel compound compliant mechanism

Guiding accuracy Δx_C [µm] on the vertical displacement of Δy_C = 5 mm		
Input force case F_a	Input force case F_b	Input force case F_c
5.1	0.95	1.2

5. MOBILITY OF THE COMPLIANT SCOTT-RUSSEL MECHANISMS

First, an experimental analysis of the flexural strength of a sample of the link with a circular flexure hinge manufactured of pyacryl (Fig. 6) was conducted [25].

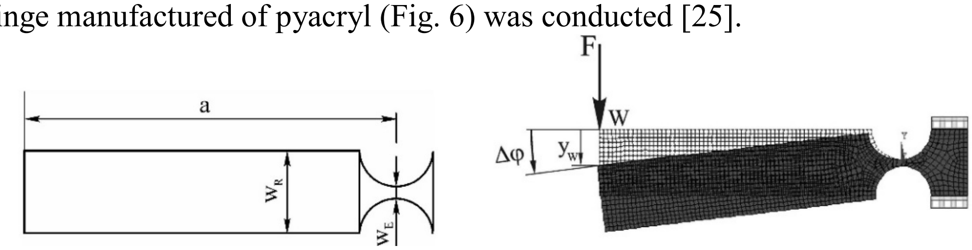

a) b)

Fig. 6. A link with notch flexure hinge in the undeformed and deformed position

The ability to utilize ANSYS Software in the displacement and stress calculation of links with flexure hinges and compliant mechanisms in the elastic area of the flexural strain (σ_{max} = 0 to 65 N/mm^2) is demonstrated by the comparison of experimentally and numerically obtained data as well as in the hyper-elastic area of the flexural strain (σ_{max} = 65 to 90 N/mm^2).

For the values $\sigma_{max} > 90$ N/mm^2, the material begins to be plastically deformed. There are significant differences between the experimental and numerical results, demonstrating that ANSYS Software cannot be utilized in the plastic region of the flexural strain for the displacement and stress calculation of links with flexure hinges and compliant mechanisms.

Due to the elastic segments' elasticity, Scott-Russel mechanisms with flexure hinges can achieve only minor displacements. In other words, they have restricted movement. ANSYS software has been used to research mobility's limitations. The links are assumed to be made of piacryl with the above-mentioned material properties (Young's modulus E = 3700 N/mm^2, flexural strength σ_{bs} = 90 N/mm^2, the thickness of material δ = 4 mm). The constraint positions of the links, in other words, the limits of angular displacement (mobility) and maximal bending force, have been determined by the condition $\sigma_{max} < \sigma_{bs}$.

The results have been shown in Table 3.

Table 3. Mobility of the compliant Scott-Russel mechanisms

Mobility			
The Compliant Scott-Russel Mechanism	**Input force case F_a**	**Input force case F_b**	**Input force case F_c**
Single (Fig. 3a)	Δy_C = 11.39 mm Δx_C = 384 µm F_{max} = 1.1 N	Δy_C = 12.04 mm Δx_C = 93.6 µm F_{max} = 0.49 N	Δy_C = 11.63 mm Δx_C = 475 µm F_{max} = 0.41 N
Compound (Fig. 5a)	Δy_C = 10.04 mm Δx_C = 10.3 µm F_{max} = 0.98 N	Δy_C = 9.78 mm Δx_C = 1.8 µm F_{max} = 0.96 N	Δy_C = 10.03 mm Δx_C = 2.3 µm F_{max} = 0.34 N

The best mobility (maximal constraint positions of the links) has been provided by the compound compliant Scot-Russel mechanism with the acting points of input load forces located in the middle of the "input crank" – A_0A and A'_0A'. However, the mobility of the compound compliant Scot-Russel mechanism with the acting points of input load forces located in the middle of the "coupler" AB - F_b and F'_b is similar to the previous one (Δy_C = 9.78 mm ≈ 10.04 mm) but has considerably better guiding accuracy (Δx_C = 1.8 µm < 10.3 µm).

6. THE COMPLIANT SCOTT-RUSSEL MECHANISMS WITH UNDERCUT FLEXURE HINGES

If the focus is on the shape of flexure hinges with notch there are two subgroups: symmetrical and asymmetrical flexure hinges [17]. In this paper's first part, we explored the effect of symmetric flexure hinges with a circular notch on rectilinear guiding. If we look for the most similar asymmetrical flexure hinge, the flexure hinge with an undercut notch can almost exactly resemble a circular notch in the symmetrical subgroup (Fig. 7).

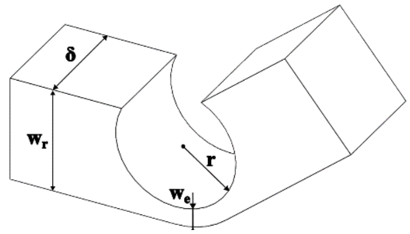

Fig. 7 The undercut flexure hinges

The undercut flexure hinge's unique shape, as seen in Fig .7, opens a path to new features of flexure hinges in general. The improvement of compliant mechanisms is defined by a change in the position of flexure hinges relative to the initially set position of joints, and this feature disallows the geometry of flexure hinges as a factor in doing so, contrary to the idea behind the synthesis of compliant mechanisms used in chapters 2 and 4.

To be able to analyze this feature, all geometrical influences of flexure hinges and compliant mechanism, need to be neutralized except the positional movement of undercut flexure hinges. This was achieved through the complete remodeling of the Scott-Russel compliant mechanism and its compound counterpart:

1) Fixing segments from joints A_0 and B to points A_{10} and B_{10} of compliant mechanism so that they cannot interfere with undercut hinge movement,
2) By placing flexure hinges with a circular notch in the places of the fixed supports A_0 and joint B (Fig. 8),
3) By moving the position and extending the rigid member BC of the compliant mechanisms (Fig. 8).

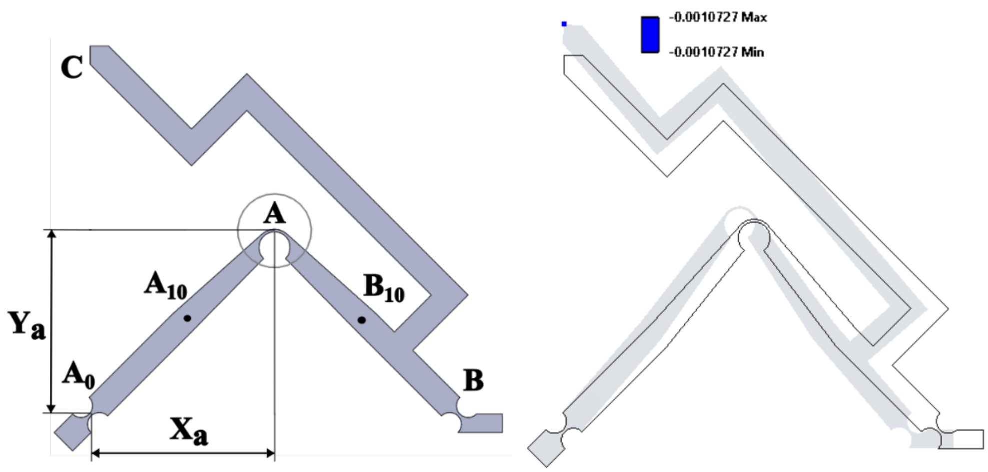

Fig. 8 The compliant Scott-Russel mechanism with undercut flexure hinges: (a) Parameters of interest, (b) Deformed and undeformed position of compliant mechanism

Because they are utilized in locations where there are opportunities for permitted movement, which is crucial in the subsequent analysis, the undercut flexure hinges are not placed on the placements of joints A_0 and B. If not, there would be a significant departure from the mechanism's original design.

Positional optimization's primary focus will be on the displacement of the undercut flexure hinges, which was parameterized in both the X (represented as Xa for the compliant Scott-Russel mechanism in Fig. 8 and analogous to that Xa_1 and Xa_2 for the compound compliant Scott-Russel mechanism) and Y (represented as Ya for the compliant Scott-Russel mechanisms in Fig. 8 and analogous to that Ya_1 and Ya_2 for the compound compliant Scott-Russel mechanism) directions. For both undercut flexure hinges, these displacement measurements were established retroactively from the locations of the fixed supports A_0 and joint B to the center of the neutral axis of the undercut hinge notch.

7. FEA AND POSITION OPTIMIZATION OF THE COMPLIANT SCOTT-RUSSEL MECHANISMS

The geometric constraint of every flexure hinge and the compliant mechanism must be completely described to do FEA and positioning optimization. In addition to the previously described geometric restrictions, it is important to provide the mechanism's static and dynamic properties. These restrictions are represented by the boundary conditions (fixed supports A and B for the single compliant Scott-Russel mechanism and A, B, E, and D for the compound Scott-Russel mechanism) and the required displacement Δy_C (C) in Fig. 9.

Using the "Refinement" function and choosing just quadratic elements, a refined mesh of finite elements is created at the places of flexure hinges (see Fig. 9). The resulting mesh was composed for the Scott-Russel single compliant mechanism of 21119 elements and 22392 nodes and the Scott-Russel compound compliant mechanism of 41590 elements and 44061 nodes. Subjected to convergence accuracy of displacement along the x-axis FE model produced error results of less than 0.5%. Again, piacryl was used as material.

The next step is to define the parameters for the position optimization after the analysis and simulation of the compliant mechanism model have been successfully defined.

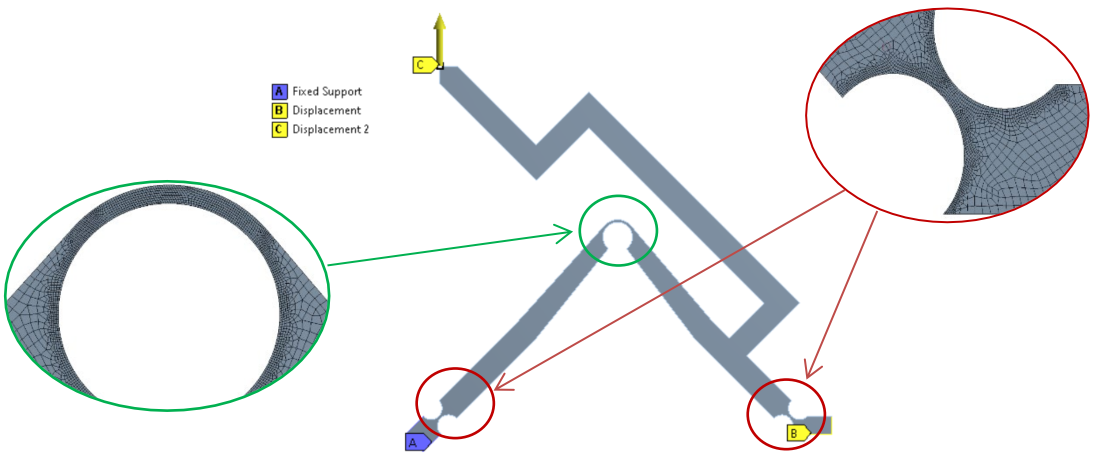

(a)

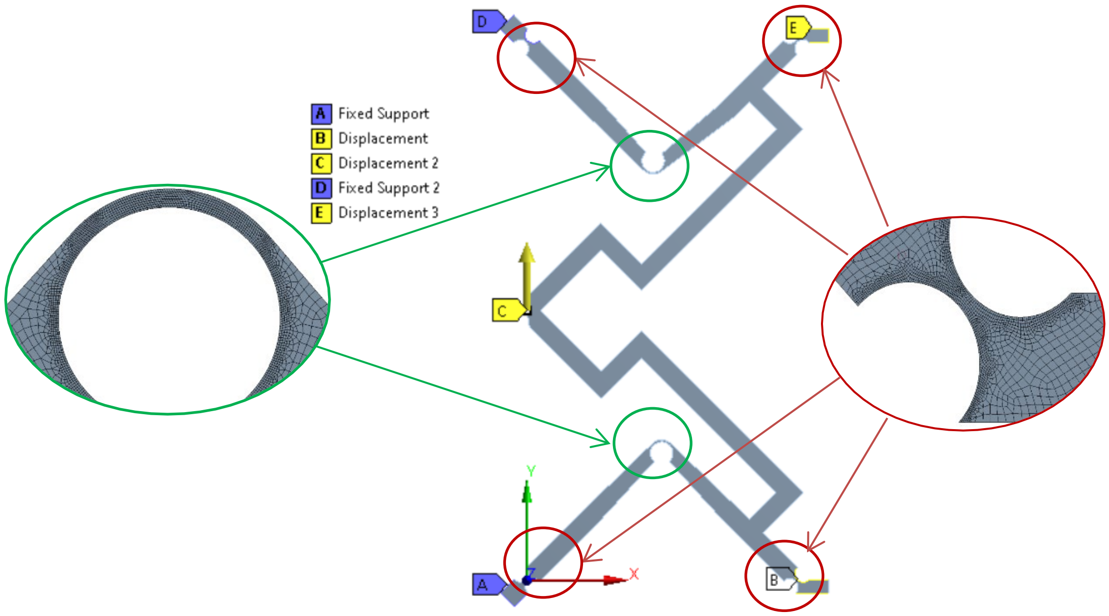

(b)

Fig. 9. The boundary conditions with finite element structure of (a) The single compliant Scott-Russel mechanism and (b) The compound compliant Scott-Russel mechanism

Optimization aims to determine the optimal position of the undercut flexure hinges. Only the values of parasitic displacement along the x-axis and elastic strain were represented as the optimization output parameters. As two parameters are required for positioning of one joint (positioning in a vertical and horizontal direction), this model, therefore, has four input parameters (Fig. 5):

1) Displacement of the undercut flexure hinge A' in the X direction (P1)
2) Displacement of the undercut flexure hinge A' in the Y direction (P2)
3) Displacement of the undercut flexure hinge A in the X direction (P3)
4) Displacement of the undercut flexure hinge A in the Y direction (P4)

Note that the Scott-Russel compliant mechanism has just two input parameters P1 and P2. In addition to the names of the input and output parameters, the characters in parentheses also serve as the parameters' ANSYS identifications. For this input parameter, it was necessary to set the minimum and maximum limits within which the parameters can alter (represented as a grey circle in Fig. 8). As all parameters have the same starting value, limits are given as 80% and 120% of starting value for minimum and maximum limits.

Based on the sensitivity analysis a quadratic parameter determination matrix is obtained. The influence of input parameters can be seen more clearly in Fig. 10 which provides an overview table segment with details on important parameter influence. Although not all parameters show a major influence on the rectilinear guidance error, all input parameters are included in the positional optimization. For instance, the influence of parameter P1 (position of undercut flexure hinge along the x-axis) on the guiding accuracy Δx_C is approximately 0.46199, and the influence of parameter P2 (position of undercut flexure hinge along the y-axis) is approximately 0.61538 in the case of the single compliant Scott-Russel mechanism (presented with a blue square in Fig. 10a). In Fig. 10b, in the case of the compound compliant Scott-Russel mechanism, you can see meager results where the values of the input to the output parameters range from minimal 0.1552 to maximal 0.26599, which will later have a negative impact on the optimization results (presented with blue square in Fig. 10b).

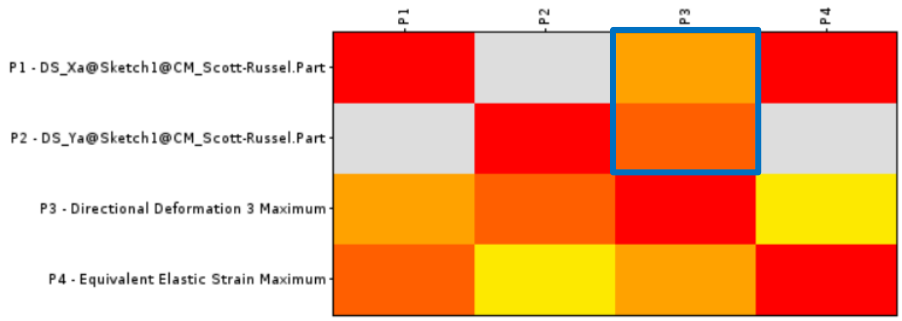

(a)

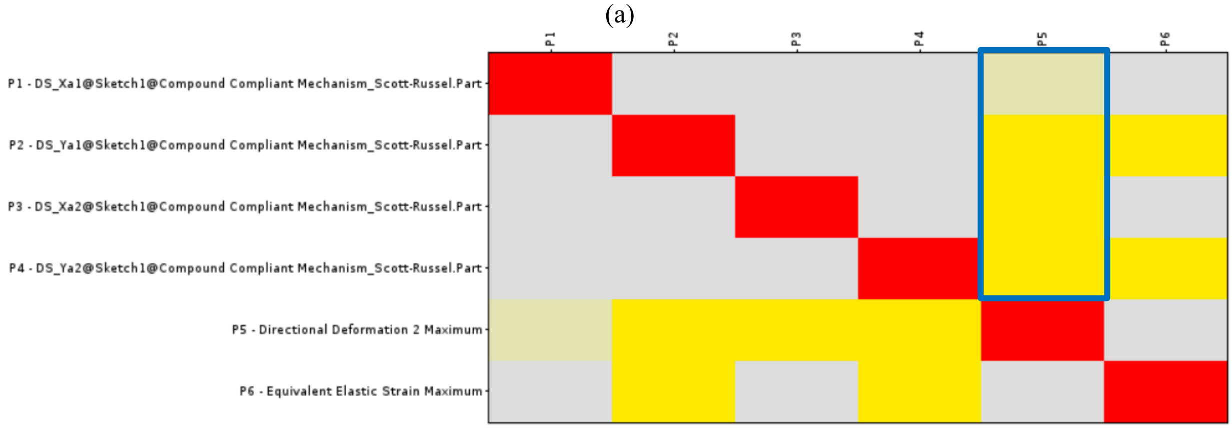

(b)

Fig. 10 Quadratic determination matrix for: (a) The compliant single Scott-Russel mechanism (input parameters P1 and P2 and output parameters P3 and P4) and (b) The compound compliant Scott-Russel mechanism (input parameters P1, P2, P3, and P4 and output parameters P5 and P6)

The reduction of point C's (in the case of both a single compliant mechanism and a compound compliant mechanism) parasitic displacement along the x-axis Δx_C (parameters P3 and P5 in Fig. 11) was the goal. The MOGA optimization method is chosen in the "Response Surface Optimization" section. Following optimization, three sets of dimensions (candidate points) are presented that best satisfy the stated objectives and restrictions (Fig. 11). Verification reveals that point candidate number three satisfies the requirements in both cases (Fig. 11).

Optimization Study						
Seek P3 = 0 mm	Goal, Seek P3 = (Default Importance)					
Optimization Method						
MOGA	The MOGA method (Multi-Objective Genetic Algorithm) is a variant of the popular NSGA-II (Non-dominated Sorted Genetic Algorithm-II) based on controlled elitism concepts. It supports multiple objectives and constraints and aims at finding the global optimum.					
Configuration	Generate 2000 samples initially, 400 samples per iteration and find 3 candidates in a maximum of 20 iterations.					
Status	Converged after 3452 evaluations.					
Candidate Points						
	Candidate Point 1	Candidate Point 1 (verified) DP 297	Candidate Point 2	Candidate Point 2 (verified) DP 298	Candidate Point 3	Candidate Point 3 (verified) DP 299
P1 - DS_Xa@Sketch1@CM_Scott-Russel.Part	34.469		31.463		35.891	
P2 - DS_Ya@Sketch1@CM_Scott-Russel.Part	38.264		35.552		39.554	
P3 - Directional Deformation 3 Maximum (mm)	-1.9075E-05	-0.0037796	5.8299E-05	-0.0030149	6.403E-05	-0.0010727

(a)

Optimization Study						
Seek P5 = 0 mm	Goal, Seek P5 = (Default Importance)					
Optimization Method						
MOGA	The MOGA method (Multi-Objective Genetic Algorithm) is a variant of the popular NSGA-II (Non-dominated Sorted Genetic Algorithm-II) based on controlled elitism concepts. It supports multiple objectives and constraints and aims at finding the global optimum.					
Configuration	Generate 4000 samples initially, 800 samples per iteration and find 3 candidates in a maximum of 20 iterations.					
Status	Converged after 8398 evaluations.					
Candidate Points						
	Candidate Point 1	Candidate Point 1 (verified) DP 588	Candidate Point 2	Candidate Point 2 (verified) DP 589	Candidate Point 3	Candidate Point 3 (verified) DP 590
P1 - DS_Xa1@Sketch1@Compound Compliant Mechanism_Scott-Russel.Part	32.267		36.949		32.906	
P2 - DS_Ya1@Sketch1@Compound Compliant Mechanism_Scott-Russel.Part	37.538		36.539		34.577	
P3 - DS_Xa2@Sketch1@Compound Compliant Mechanism_Scott-Russel.Part	31.865		33.122		35.331	
P4 - DS_Ya2@Sketch1@Compound Compliant Mechanism_Scott-Russel.Part	37.149		33.334		36.619	
P5 - Directional Deformation 2 Maximum (mm)	-2.8729E-06	0.0010763	2.5986E-05	0.0087844	-2.7551E-05	0.00013665

(b)

Fig. 11 Candidate points determined based on the MOGA method: (a) The single compliant Scott-Russel mechanism and (b) The compound compliant Scott-Russel mechanism

The outcomes unequivocally demonstrate an increase in the underlying mechanism's (the Scott-Russel four-bar mechanism) operational correctness.

Table 4. Obtained candidates with parameter correlation

Guiding accuracy Δx_C [µm] on the vertical displacement of Δy_C = 5 mm	
The single compliant Scott-Russel mechanism	1.0727
The compound compliant Scott-Russel mechanism	0.13665

6. CONCLUSION

The most common way to create a compliant mechanism is to build it as the counterpart of a rigid-body linkage that can perform the desired function (also known as the rigid-body replacement approach). The design of the compliant cognate four-bar linkages has been introduced in this study. As alternatives to the rigid-body Scott-Russel mechanism, which allows the coupler point to be steered on an exact rectilinear path, the basic compliant mechanism and compound compliant mechanisms have been created.

For all of the aforementioned compliant mechanisms that can realize approximate rectilinear guiding of the coupler point, the guiding accuracy, or the difference between the realized and exact rectilinear trace, as well as the mobility, or determining the constraint position of the links, have been analyzed and compared.

The compliant Scott-Russel mechanism with circular flexure hinges notch and the acting point of input load force situated in the middle of the "coupler" AB, has provided the highest guiding accuracy (minimum variation between absolute rectilinear and realized trace) of the "coupler" point on the rectilinear trace Δx_C = 92,6 µm. Better results were obtained for this mechanism with the help of undercut flexure hinges and position optimization, which gives us a model with a guidance accuracy of Δx_C = 1.0727 µm.

On the other hand, the best mobility (maximal constraint positions of the links) has been provided by the compound compliant Scott-Russel mechanism with the acting point in the middle of the "coupler" AB with a guidance accuracy of Δx_C = 0.95 µm. Position optimization and undercut flexure hinges improved the performance of this compound compliant mechanism with a guidance accuracy of Δx_C = 0.13665 µm.

The results of guiding accuracy, as well as mobility offered by the cognate compliant mechanisms, should be taken into consideration in the synthesis procedure of the compliant mechanisms. Likewise, FEA and position optimization should also be bear in mind in the synthesis of compliant mechanisms.

Acknowledgment: *This research was financially supported by the Ministry of Education, Science and Technological Development of the Republic of Serbia (Contract No. 451-03-47/2023-01/200109).*

REFERENCES

[1] Aboulissane B, El Bakkali L, El Bahaoui J (2020) Workspace analysis and optimization of the parallel robots based on the computer-aided design approach. Facta Universitatis, Series Mechanical Engineering 18(1):079-089

[2] Aboulissane B, El Haiek D, El Bakkali L, El Bahaoui J (2019) On the workspace optimization of parallel robots based on CAD approach. Procedia Manufacturing 32:1085-1092

[3] Yang ZG, Shao ML, Shin DI (2015) Kinematic optimization of parallel manipulators with a desired workspace. In Applied Mechanics and Materials, Trans Tech Publications Ltd 752:973-979

[4] Tsirogiannis E, Vosniakos G (2019) Redesign and topology optimization of an industrial robot link for additive manufacturing. Facta Universitatis, Series Mechanical Engineering 17(3):415-424

[5] Junk S, Klerch B, Nasdala L, Hochberg U (2018) Topology optimization for additive manufacturing using a component of a humanoid robot. Procedia Cirp 70:102-107

[6] Fetisov KV, Maksimov PV (2018) Topology optimization and laser additive manufacturing in the design process of efficiency lightweight aerospace parts. In Journal of Physics: Conference Series, IOP Publishing 1015 (5):052006

[7] Fragassa C (2021) Lightening structures by metal replacement: from traditional gym equipment to an advanced fiber-reinforced composite exoskeleton. Facta Universitatis, Series Mechanical Engineering:155-174

[8] Both J, Morasch A, Wehrle E, Baier H (2011) Advanced manufacturing and design techniques for lightweight structures. International Aluminium Journal 87:60-64

[9] Heggemann T, Homberg W (2019) Deep drawing of fiber metal laminates for automotive lightweight structures. Composite Structures 216:53-57

[10] Zentner L, Linβ S (2019) Compliant systems - Mechanics of elastically deformable mechanisms, actuators and sensors. De Gruyter, Oldenbourg, Muenchen

[11] Howell LL, Magleby SP, Olsen BM (2013) Handbook of Compliant Mechanisms. John Wiley & Sons Inc., New York

[12] Howell LL (2001) Compliant mechanisms. John Wiley &Sons, Inc., New York

[13] Midha A, Norton TW, Howell LL (1994) On the nomenclature, classification, and abstractions of compliant mechanisms. ASME Journal of Mechanical Design 116 (1):270-279

[14] Howell LL, Midha A (1994) Method for the design of compliant mechanisms with small-length flexural pivots. ASME Journal of Mechanical Design 116 (1):280-290

[15] Ananthasuresh GK, Kota S (1995) Designing compliant mechanisms. Mechanical Engineering 117 (11): 93-96

[16] Böttcher F, Christen G, Pfefferkorn H (2001) Structure and function of joints and compliant mechanism. Motion Systems (Collected Short Papers of the Innovationskolleg “Bewegungssysteme” Friedrich-Schiller Universität Jena), Technische Universität Jena, Technische Universität Ilmenau, ShakerVerlag, Aachen: 30-35

[17] Pavlović ND, Pavlović NT (2013) Compliant mechanisms (in Serbian). Faculty of Mechanical Engineering, University of Niš, Serbia

[18] Pavlović NT, Pavlović ND (2003) Motion characteristics of the compliant four-bar linkages for rectilinear guiding. Journal of Mechanical Engineering Design (Yugoslav Society for Machine Elements and Design) 6 (1):20-27

[19] Pavlović NT, Pavlović, ND (2004) Rectilinear guiding accuracy of Roberts-Chebyshev compliant four-bar linkage with silicone joints. Mehanika na mašinite 12 (4):53-56

[20] Pavlović NT, Pavlović ND, Milošević M (2016) Selection of the optimal rigid-body counterpart mechanism in the compliant mechanism synthesis procedure. Microactuator and Micromechanisms, Proceedings of MAAM, Ilmenau, Germany, October 5-7, 2016, Springer:127-138

[21] Pavlović NT, Pavlović ND (2009) Compliant mechanism design for realizing of axial link translation. Mechanism and Machine Theory 44(5):1082-1091

[22] Pavlović NT, Stojiljković D (2022) Guiding accuracy of the Watt compliant cognate mechanisms. Facta Universitatis, Series: Mechanical Engineering. https://doi.org/10.22190/FUME220822044P. Preprint at http://casopisi.junis.ni.ac.rs/index.php/FUMechEng/article/view/11038

[23] Yuan Y, Ren J, Wang Z, Mu X (2022) Dynamic analysis of the rigid-flexible excavator mechanism based on virtual prototype. Facta Universitatis, Series: Mechanical Engineering 20(2):341-361

[24] Stojiljković, D., Pavlović, N.T., Milošević, M. (2022). Design of Compliant Mechanism for Rectilinear Guiding with Non-conventional Optimization of Flexure Hinges. In: Khang, N.V., Hoang, N.Q., Ceccarelli, M. (eds) Advances in Asian Mechanism and Machine Science. ASIAN MMS 2021. Mechanisms and Machine Science, vol 113. Springer, Cham. https://doi.org/10.1007/978-3-030-91892-7_35

[25] Pavlović NT, Pavlović ND (2005) Mobility of the compliant joints and compliant mechanisms. Theoretical and Applied Mechanics, Belgrade 32 (4):341-357

CONTACTS

Dušan Stojiljković — email: dusan.stojiljkovic@masfak.ni.ac.rs
ORCID: https://orcid.org/0000-0002-6787-4533

Prof. Dr.-Ing. Nenad T. Pavlović — email: nenad.t.pavlovic@masfak.ni.ac.rs
ORCID: https://orcid.org/0000-0001-5986-5023

